24th COBEM - 2017

24th ABCM International Congress of Mechanical Engineering
December 3-8, 2017, Curitiba, PR, Brazil

COBEM-2017-0621
NUMERICAL/EXPERIMENTAL ANALYSIS OF THE CRACK TRAJECTORY IN MIXED-MODE LOADING

André Luis Pinto
Jorge Luiz de Almeida Ferreira
University of Brasilia, Department of Mechanical Engineering, Brasilia, Brazil
andreluiseng.mecanica@gmail.com, jorge@unb.br

Abstract. *It is important to be able to predict the fatigue life of mechanical components with the objective of avoiding premature exchange of such components. However, this is not trivial when the component is subject to mixed-mode loading. The presence of stress intensity* K_I *and* K_{II} *cause changes in the direction of crack propagation. This work proposes a routine for predicting the crack trajectory in a finite element software (Ansys APDL), where the slope of the crack is calculated by the MCS (Maximum circumferential stress) model. The da/dN x ΔK curves of the 7050-T7451 aluminum alloy were experimentally obtained for various lamination directions in the fatigue laboratory of the UnB, based on these results the numerical simulations were performed. The methodology is validated with experimental results obtained through fatigue tests on modified compact tension CT specimens, in which holes were machined to curve the crack propagation path. The method used shows excellent results for the CT with the direction of lamination S-L, but for the directions T-L and T-S did not obtain good predictions.*

Keywords: *Fatigue crack growth, Finite elements, Maximum circunferential stress.*

1. INTRODUCTION

It is fundamental to study phenomena such as the initiation and propagation of cracks for the preparation of maintenance and inspection plans in any area of engineering. The importance of knowledge of the mechanical behavior of fractured equipment reflects the financial return, avoiding considerable expenses. The life of a mechanical component can be increased safely, thus causing a reduction in the number of maintenance intervals (Mandai, 2010).

One of the great problems that society has been dealing with since the first structural constructions is the existence of fractured components. Currently, with equipment that is more complex and the requirement of more secure systems the problem is even greater (Castro, 2013). “Duga, et al., 1983” carried out a study which gives an insight into the importance of Fracture Mechanics. It estimated an annual cost of $119bi a year from fractured mechanical components, about 4% of US gross domestic product in 1978. It could be reduced by $35bi if applied all knowledge at the time of fatigue failure, and $28bi also applied the theory of Fracture Mechanics.

The design of aircraft are made using models based on damage tolerance approach, and often require the prediction of mixed-mode fatigue crack growth. In these cases, the crack path becomes an essential aspect for the fatigue life simulation using the methodology of fracture mechanics. However, most of the existing approaches are limited to the mode I fatigue crack growth cases (Blažić, *et al*, 2014).

A more accurate way of modelling crack propagation in a finite element mesh is to modify the part and to perform automatic re-meshing. Several methods have been proposed in the literature to model without any re-meshing. However, these recent techniques still have to be improved in order to deal with complex configurations such as multiple cracks, large deformation crack propagation, etc. When re-meshing is possible, this method for representing the crack growth seems to be more accurate (Boulenouar, *et al*, 2014).

For the manufacture of aircraft, it is very common to use aluminum alloy plates in the assembly of the airplane's fuselage. However, during the assembly process, which is done by fixing the plates by rivets, microscopic cracks are generated close to the rivets. Due to the importance of the application of alloy Al 7050-T7451, the data obtained by (Almeida, 2016) were used in tests carried out in the laboratories of UnB for this alloy in the accomplishment of numerical simulations with Ansys software. The validation of the method is done using crack propagation tests under constant loading on modified compact tension CT specimens, in which holes were machined to curve the crack propagation path.

2. FRACTURE MECHANICS

When the usual methods for structural calculation became insufficient to solve problems such as failure of structures requested by loads below the permissible stresses the Fracture Mechanics developed. Fracture mechanics basically studies the phenomena involved in the propagation of cracks and is divided into two branches: the one governed by the linear-elastic behavior (LEFM) and the one governed by elastoplastic behavior (EPFM) (Rosa, 2002).

Linear-elastic fracture mechanics is used in cases where the fracture occurs without extensive plastic deformation. This can occur due to material properties, geometry or if the temperature is sufficiently low. However, most of the materials used in mechanical designs have considerable plasticity. For these cases, the Elastoplastic Fracture Mechanics is applied. Within the mechanics of elastoplastic fracture are two main methods of evaluation, the CTOD (Crack tip opening displacement) technique and the *J*-integral (Dowling, 2013).

There are three distinct ways of propagating a crack, as shown in Fig. 1. A traction load gives rise to mode I, the crack opening propagation mode, being the most common. Mode II is the sliding mode, a result of the shear in the plane. Mode III is the tear mode, result of shearing out of the plane. (Budynas and Nisbett, 2011).

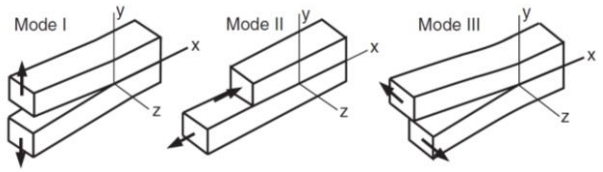

Figure 1. The basic modes of crack surface displacement. (Dowling, 2013).

That is why the universal notation of K_I for the stress intensity factor in the crack opening mode I. For other modes the corresponding stress intensity factor is called K_{II} and K_{III}. In 1957, G.R. Irwin showed that the stress intensity factor on a plate with a crack is determined by Eq. (1). Where, σ is the normal tension of traction, F is the form factor and a is the length of the crack.

$$K_I = \sigma F \sqrt{\pi a} \tag{1}$$

2.1 Fatigue crack propagation

Fatigue failures are a major cause of failure in mechanical components. Because these components are subjected to durable cyclic loading, they fail even when loaded by tension below the mechanical tensile strength of the material. The study of fatigue can be performed in an approach with emphasis on stress or deformation, and countless variables can influence the strength of the material (Santos, 2013). The Fig. 2 represents the most common types of fatigue loads.

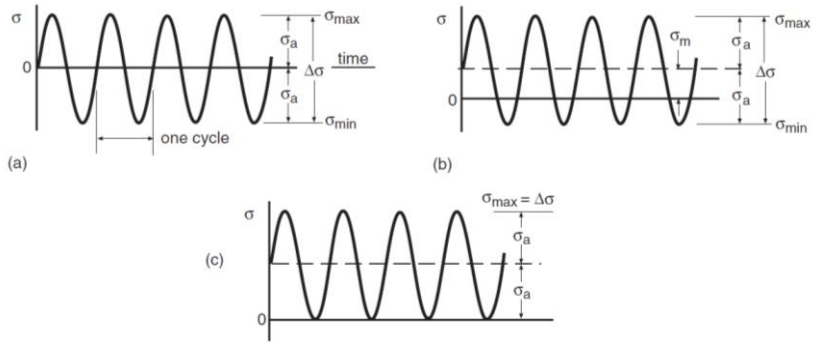

Figure 2. Constant amplitude cycling and the associated nomenclature. Case (a) is completely reversed stressing; (b) as a nonzero mean stress; and (c) is zero-to-tension stressing (Dowling, 2013).

Some relationships between stresses are:

$$\sigma_m = (\sigma_{\max} + \sigma_{\min})/2; \text{ } \textit{Medium stress} \tag{2}$$

$$\sigma_a = (\sigma_{\max} - \sigma_{\min})/2; \text{ } \textit{Alternating stress} \tag{3}$$

$$R = \sigma_{\min} / \sigma_{\max}; \text{ Loading Ratio} \quad (4)$$

In newly manufactured parts, it is unusual to find cracks with significant sizes, only micro defects that can be aggravated with the requests in time. It is known that the presence of a crack in a mechanical component reduces its mechanical resistance and consequently its useful life. As shown in Fig. 3, the crack propagation initially occurs with a plastic deformation at the tip of the crack upon being charged, upon being discharged or even compressed, the crack is returned to be pointed and raising the concentration of local stresses. Slip of crystal planes along directions of maximum shear occurs as indicated by arrows, and this plastic blunting process results in one striation (Δa) being formed for each cycle (Downling, 2013).

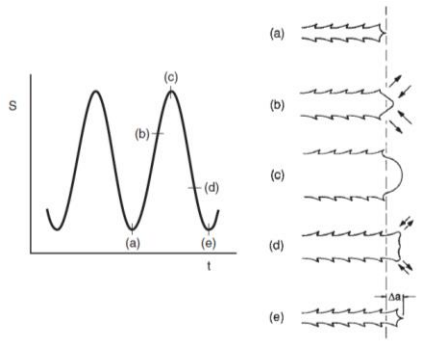

Figure 3. Hypothesized plastic deformation behavior at the tip of a growing fatigue crack during a loading cycle (Dowling, 2013).

To avoid catastrophic failures in engineering it is important to know how fast a crack is growing. Due to the relationships between the crack length and the stress intensity factor K, it is possible to associate a crack growth Δa, with a ΔK. By means of experiments it is possible to observe that a crack grows a small amount with each cycles of loads N, and the greater the magnitude of this loading, the faster the crack growth. Thus it is possible to estimate the rate of crack growth as a function of ΔK (Santos, 2013). Fig. 4 is representing a curve $da/dN \times \Delta K$ raised experimentally in log-log scale.

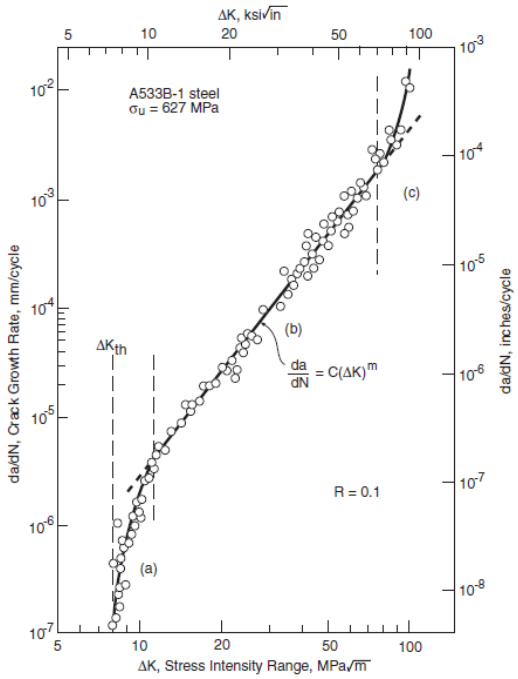

Figure 4. Fatigue crack growth rates over a wide range of stress intensities for a ductile pressure vessel steel (Dowling, 2013).

As shown in the Fig. 4, the curve can be divided into three stages. In the first we have a threshold value ΔK_{th}, where the crack growth is considered slow, within the second stage the propagation is considered stable and can be

related to several mathematical models, and in the third stage the crack growth occurs in an unstable form and the fracture can occur at any time. In cases where the plastic zone is small enough, the value of K in the third stage coincides with the value of the fracture toughness, K_{Ic} (Santos, 2013).

As described previously, in stage two the rate da/dN can be modeled as a function of factor ΔK. Paris and Erdogan (1903) developed the following equation for the crack growth rate (Dowling, 2013):

$$\frac{da}{dN} = C(\Delta K)^m \tag{5}$$

In which *C* is a constant and *m* is the slope of the curve in stage two. These two parameters are obtained experimentally for each type of material, this is done by applying a log-log linear regression. In general the value of *m* can vary between 2 and 4 for metallic materials (Dowling, 2013).

3. *J*-INTEGRAL

Rice developed the *J*-integral method, for the evaluation of fracture toughness considering a material of non-linear elasticity, as shown in Fig. 5. *J*-integral is a line integral that does not depend on the path and measures the resistance of singular stresses and deformations near the crack tip (Mandai, 2010).

$$J = \int_{\Gamma} \left(w dy - T_i \frac{du_i}{dx} ds \right) \tag{6}$$

According to Eq. (6), Γ is a closed and anticlockwise contour defined on a normal plane the front of the crack starting at the lower face of the crack and ending at the upper face, represented by Fig. 6. *w* is the strain energy density. T_i and u_i are the cartesian components of the traction vector and displacement vector in the coordinate system the front of the crack (Savioli, 2011).

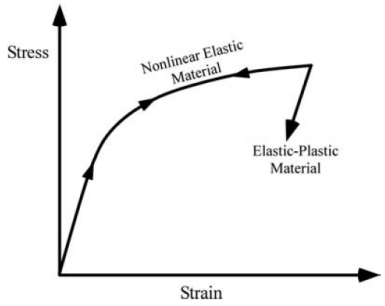

Figure 5. Schematic comparison of the stress-strain behavior of elastic-plastic and nonlinear elastic materials (Anderson, 2005).

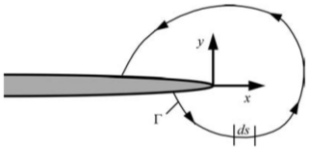

Figure 6. Arbitrary contour around the tip of a crack (Anderson, 2005).

For a linear elastic material we can obtain a relation between the *J*-integral and the rate of energy release G, where $J = G$.

$$J = \frac{K_I^2}{E} \text{ (for a plane stress state)} \tag{7}$$

$$J = \frac{(1-\nu^2)K_I^2}{E} \text{ (for plane strain state)} \tag{8}$$

4. MAXIMUM CIRCUMFERENTIAL STRESS

There are at least three criteria widely used to predict the path of fatigue cracks. The maximum circumferential stress, the maximum potential energy release rate, and the minimum strain energy density (Miranda, *et al.*, 2003). These three methods generate similar results when used to predict the path of fatigue cracks (Bittencourt, *et al.*, 1996).

The criterion of maximum circumferential stress is the most simple, so it was chosen to be implemented in this work. This criterion assumes that the cracks grow in a direction perpendicular to the maximum normal tensile stress in front of the crack tip, this tension tends to open the faces of the crack avoiding the friction between them, thus the plastic work to generate and propagate the plastic zones in the crack tip are minimized (Castro e Meggiolaro, 2009).

For a general case of mixed load the direction of the crack increment is given by:

$$\theta = 2\arctan\left(\frac{K_I}{4K_{II}} \pm \frac{1}{4}\sqrt{\left(\frac{K_I}{K_{II}}\right)^2 + 8}\right) \tag{9}$$

The angle θ is the angle between the plane of the initial propagation and the original plane of the requested crack in mixed mode. Under pure mode I, $K_{II} = 0$ and $\theta = 0°$, the crack remains in its plane. However, if the crack is subjected to the pure mode II, $K_I = 0$ and $\theta = \pm 70{,}5°$. The angle signal θ depends on K_{II}: for $K_{II} > 0 \Rightarrow \theta < 0$, and for $K_{II} < 0 \Rightarrow \theta > 0$.

5. NUMERICAL METHODOLOGY

The proposed methodology was used to numerically simulate a crack propagation test in a compact tension CT specimen in terms of *ASTM E647*. However, the CTs were modified by adding a hole in their geometry as shown in Fig. 7 and 8, the dimensions are in millimeters. The routine is written in the language *APDL* (*Ansys Parametric Design Language*), where the software allows the construction of the physical model and automation of common tasks through program functions. The APDL language encompasses several tools for automating scripts such as command repetition, macros, if-then-else-type branching, loops, vector operations, arrays, and scalars.

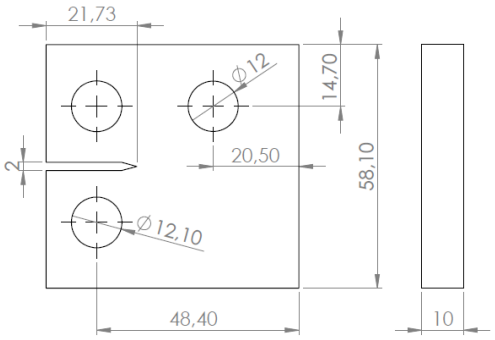

Figure 7. Dimensions of type A CT.

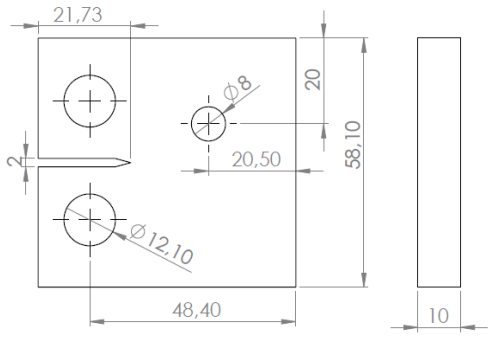

Figure 8. Dimensions of type B CT.

In the modeling we used an element recommended by the software and also used by (Jensen, 2015) called PLANE183, this is a two-dimensional element of high order with quadratic behavior that is recommended for irregular

meshes. The PLANE183 element can adapt to geometry and automatically generate meshes with quadrilateral eight-node or triangular six-node elements, as shown in Fig. 9. Each node of the element has two degrees of freedom, which are the nodal translations in the x and y directions. This element can be used as a plane element (plane stress state, plane strain state or deformation in the generalized plane) or as an axisymmetric element. The element also allows to obtain results as: nodal displacements, plastic deformation, normal stress, stress and main directions.

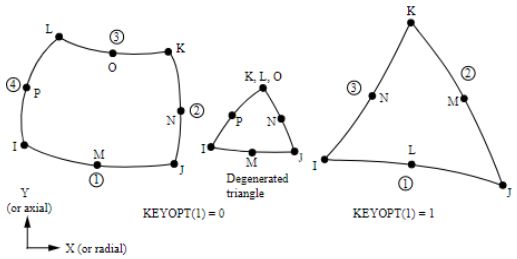

Figure 9. PLANE183 element for quadrilateral and triangular shape (Jensen, 2015).

To implement the method, the text file was created with an algorithm written in Ansys Parametric Design Language (APDL). By means of this algorithm the value of K_I and K_{II} is calculated for the established loading and pre-crack amplitude. The calculation of the stress intensity factors is done by the software by a model based on the method of *J*-integral. Using the maximum circumferential stress method, the slope increment is calculated, then the crack length is increased and a new K_I and K_{II} value is calculated for each new crack length. At the beginning of the program, the data of the material properties, the geometric characteristics, the boundary conditions, the length of the increment that the crack will propagate and the number of steps are inserted. As shown in Fig. 10, Y is defined as the distance between the two faces of the crack, INC is the size of each crack increment, and α is the angle formed by the lines at the crack tip.

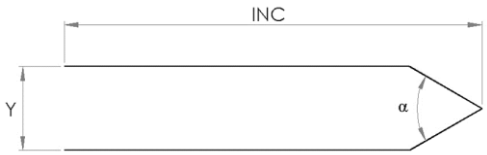

Figure 10. Idealization of the crack or increase of the crack.

To perform this procedure you must use the command **DO*. It performs the loop with *n* steps, where the stop criterion is the number of predefined cycles. The values of the stress intensity factor is calculated for each increment of crack and printed in a text file with the command **VWRITE*. The approach used in *Ansys* to predict the crack trajectory is explained in the flowchart of Fig. 11.

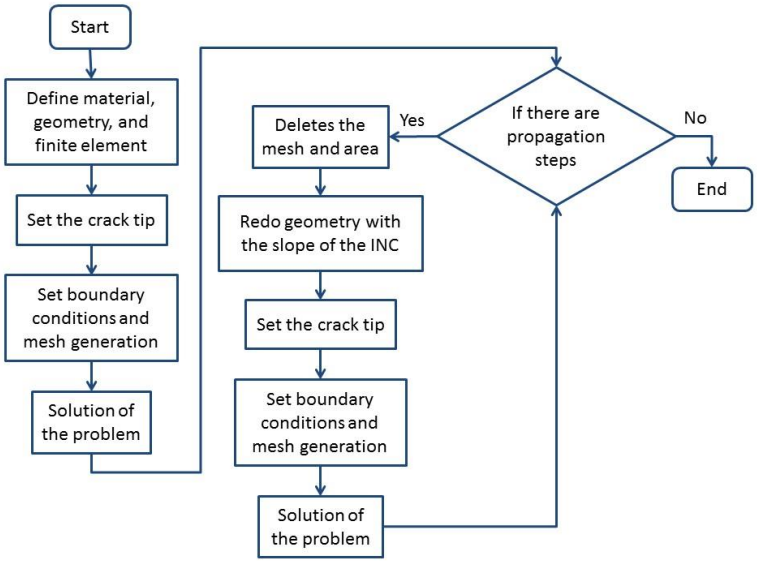

Figure 11. Flowchart of the crack trajectory prediction model.

6. RESULTS

6.1 General aspects

The experimental data for alloy Al 7050-T7451 were obtained in the fatigue laboratory of the University of Brasilia. For the numerical simulation, data from the tests performed by (Almeida, 2016) were used. In his work $da/dN \times \Delta K$ curves were raised for several directions of lamination, Fig. 12 shows the results. For the present work, data were used only for the directions of lamination S-L, T-S and T-L. Tab. 1 shows the dimensions of the specimens used in the work of (Almeida, 2016).

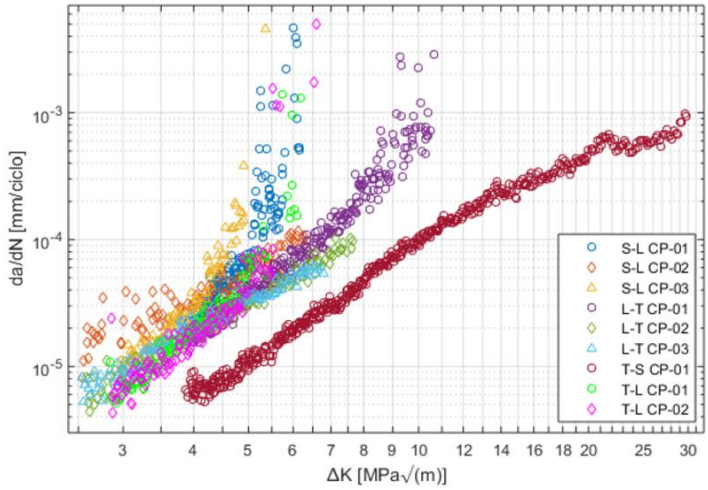

Figure 12. Curves $da/dN \times \Delta K$ of aluminum alloy 7050 T-7451 (Almeida, 2016).

Table 1. Specimen size for crack propagation (Almeida, 2016).

Component	Dimension (mm)
W	48,4
B	10
a_n	9,68
D	12,1

6.2 CT specimen 1 – Type A

The CT 01 has the direction of lamination T-S. For this test, the third bore was first performed, then the pre-crack was generated. The frequency of the loads in the pre-crack generation was $25Hz$, and during the crack propagation $30Hz$. A loading ratio was used $R = 0{,}1$ with $P_{\max} = 2.000N$. The length of the pre-crack obtained was $a = 11{,}85mm$, the K_f of the pre-crack was $5MPa\sqrt{m}$. The number of cycles until failure (encounter of the crack with the third hole) after the creation of the pre-crack was 898.727 cycles.

Fig. 13 shows the comparison between the experimental test performed with CT 01 and the simulation in *Ansys* software. The simulation shown in Fig. 13a was performed with an average mesh size of 1mm and 0,5mm increments. The initial mesh of the finite element model contained 3.657 elements and 11.185 nodes, and the final mesh with 6.052 elements and 18.484 nodes. The processing time was 46 minutes and 2,4 seconds. For this simulation was defined a thickness representing the distance between the faces of the crack of Y = 0,1mm, and the angle between the faces of the crack tip as $\alpha = 60°$.

With the parameters *C* and *m* of the Paris curve in the T-S direction obtained by (Almeida, 2016), it was possible to calculate the life with the numerical data, thus finding a value of *N* = 7.759.196 cycles. As shown by Fig. 13, the numerical trajectory shows a great difference with the trajectory obtained experimentally, consequently diverging also in the life prediction, since the life of the CT obtained in the laboratory was of *N* = 898.727 cycles.

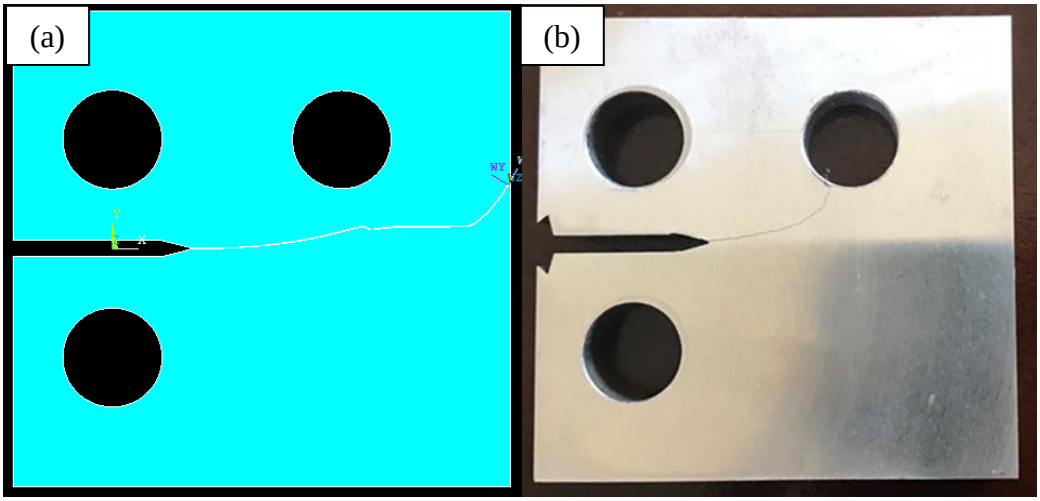

Figure 13. Trajectory of numerical (a) and experimental (b) crack of CT-01.

6.3 CT specimen 2 – Type A

The CT 02 has the direction of lamination S-L. For this test the pre-crack was first performed, and then the third bore. The frequency of the loads in the pre-crack generation was $25Hz$, and during the crack propagation $30Hz$. A loading ratio was used $R = 0{,}1$ with $P_{\max} = 2.000N$. The length of the pre-crack obtained was $a = 14{,}68mm$, the K_f of the pre-crack was $5MPa\sqrt{m}$. The number of cycles until failure (complete separation of CT) after the creation of the pre-crack was 24.765 cycles.

The simulation shown in Fig. 14a was performed with a mean mesh size of 1mm and 0,5mm increments. The initial mesh of the finite element model contained 3.589 elements and 10.991 nodes, and the final mesh with 5.888 elements and 17.974 nodes. The processing time was 38 minutes and 8.8 seconds. For this simulation was defined a thickness representing the distance between the faces of the crack of Y = 0,1mm, and the angle between the faces of the crack tip as $\alpha = 60°$.

With the parameters *C* and *m* of the Paris curve in the S-L direction obtained by (Almeida, 2016), it was possible to calculate the life with the numerical data, thus finding a value of *N* = 21.871 cycles. In the laboratory a life of *N* = 24.765 cycles was obtained, with an error of -13,26%, an acceptable result can be considered. As shown by Fig. 14, the numerically predicted path is very close to the experimental result. Figure 14b shows the numerical trajectory superimposed on the experimental trajectory, showing the similarity between the two trajectories.

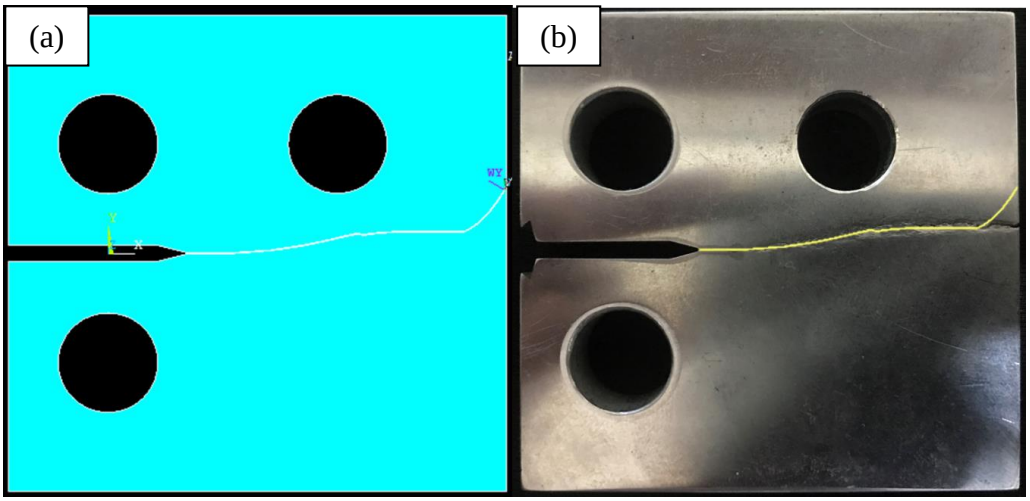

Figure 14. Trajectory of numerical (a) and experimental (b) crack of CT-02.

6.4 CT specimen 3 – Type B

The CT 03 has the direction of lamination T-L. For this test the pre-crack was first performed, and then the third bore. The frequency of the loads in the pre-crack generation was $25Hz$, and during the crack propagation $30Hz$. A

loading ratio was used $R = 0{,}1$ with $P_{max} = 2.000N$. The length of the pre-crack obtained was $a = 11{,}75mm$, the K_f of the pre-crack was $5MPa\sqrt{m}$. The number of cycles until failure (encounter of the crack with the third hole) after the creation of the pre-crack was 225.298 cycles.

The simulation shown in Fig. 15a was performed with a mean mesh size of 0,5mm and 0,5mm increments. The initial mesh of the finite element model contained 12.762 elements and 38.780 nodes, and the final mesh with 14.706 elements and 44.698 nodes. The processing time was 2 hours 43 minutes and 55.2 seconds. For this simulation was defined a thickness representing the distance between the faces of the crack of Y = 0,1mm, and the angle between the faces of the crack tip as α = 60°.

With the parameters *C* and *m* of the Paris curve in the T-L direction obtained by (Almeida, 2016), it was possible to calculate the life with the numerical data, thus finding a value of *N* = 214,314 cycles. As shown by Fig. 15, the numerical trajectory presents a great difference with the trajectory obtained experimentally, consequently diverging also in the life prediction, since the life of the CT obtained in the laboratory was of *N* = 225.298 cycles.

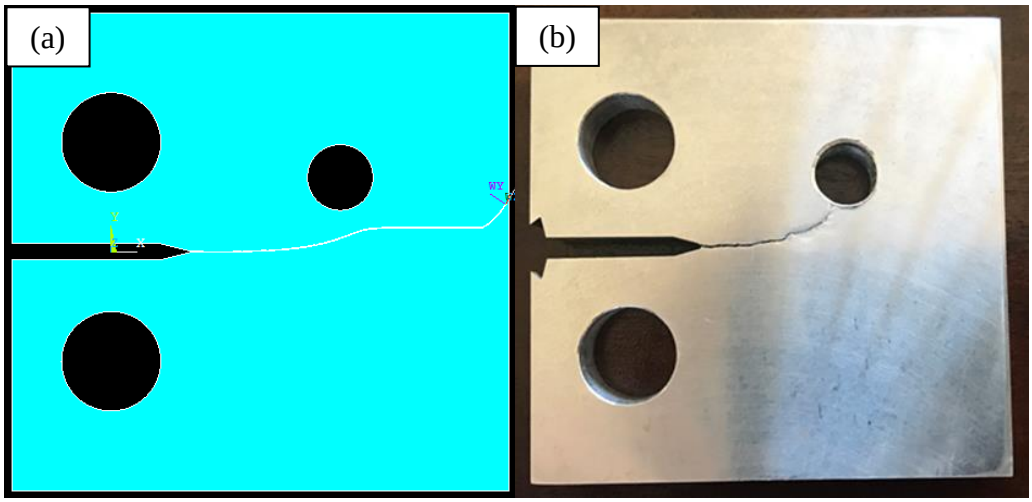

Figure 15. Trajectory of numerical (a) and experimental (b) crack of CT-03.

7. CONCLUSION

In this paper, was developed a two-phase methodology to predict fatigue crack propagation in generic 2D structures to constant amplitude loading histories. First, the finite element mesh is created and the values of the stress intensity factors are calculated along the length of the crack at each step of the propagation. Afterwards, the computed values were then used to predict the propagation fatigue life.

According to the data presented in this paper, it is concluded that the life and the trajectory of cracks in 7050-T7451 alloy specimens, oriented in the S-L directions can be satisfactorily predicted by the numerical method presented. For this case, the life prediction obtained by the numerical model gave an error of -13,26%, and the prediction of the crack trajectory was quite close to the experimental trajectory.

However, for specimens with the T-S and T-L orientation this was not possible due the tendency in deviate from the propagation plane during the crack growth, as shown by (Lemos, 2016) in his studies about the T-S direction. In these cases, the crack has a tendency of propagation in the transversal direction of lamination. This behavior is related to the effects of the lamination process, which modifies the morphological characteristics of the grains.

8. ACKNOWLEDGEMENTS

We would like to thank Msc Marcus Vinícius Costa Sá for his support in the work done in the fatigue laboratory of the University of Brasilia and CAPES for the scholarship that partially supported this research.

9. REFERENCES

Anderson, T. L., 2005. *Fracture Mechanics: Fundamentals and Aplications*. Taylor and Francis, Boca Raton, 3rd edition.

Almeida, A. F., 2016. *Avaliação do Efeito da Direção de Laminação Sobre a Taxa de Propagação de Trincas no Alumínio 7050-T7451*. Dissertação de Mestrado em Integridade de Materiais da Engenharia, Dissertação de Mestrado em Integridade de Materiais da Engenharia, Faculdade UnB Gama/FT/Universidade de Brasília, DF.

Bittencourt, T. N., Wawrzynek, P. A., Ingraffea, A., and Sousa, J. L., 1996. Quasi-automatic simulation of crack propagation for 2D LEFM problems. *Engineering Fracture Mechanics, 55*, 321-334.

Blažić, M., Maksimović, S., Petrović, Z., Vasović, I. and Turnić, D., 2014. "Determination of Fatigue Crack Growth Trajectory and Residual Life under Mixed Modes". *Strojniški vestnik - Journal of Mechanical Engineering*, Vol. 60, p. 250-254.

Boulenouar, A., Benseddiq, N., Mazari, M. and Benamara, N., 2014. "Fe Model for Linear-Elastic Mixed Mode Loading:Estimation of Sifs and Crack Propagation". *Journal of Theoretical and Applied Mechanics*, Vol. 52, p. 373-383.

Budynas, R. G., and Nisbett, J. K., 2011. *Elementos de Máquinas de Shigley: Projeto de Engenharia Mecânica*. AMGH, Porto Alegre, 8th edition.

Castro, F. R., 2013. *Avaliação do Comportamento Mecânico e Tenacidade a Fratura do Aço SAE/AISI 4140 Submetido a Tratamento Térmico Criogênico.* Dissertação de Mestrado em Engenharia e Ciência dos Materiais - Universidade Estadual Norte Fluminense Darcy Ribeiro, RJ.

Castro, J. T., and Meggiolaro, M. A., 2009. *FADIGA - Técnicas e Práticas de Dimensionamento Estrutural sob Cargas Reais de Serviço, Volume II - Propagação de Trincas, Efeitos Térmicos e Estocásticos.* CreateSpace, Estados Unidos.

Dowling, N. E., 2013. *Mechanical Behavior of Materials: Engineering Methods for Deformation, Fracture, and Fatigue*. Pearson Education, USA, 4th edition.

Duga, J. J., Fisher, W. H., Buxbaum, R. W., Rosenfield, A. R., Burh, A. R., Honton, E. J., and McMilian, S. C., Março de 1983. "The Economic Effects of Fracture in the United States". *NBS Special Publication 647-2, U.S. Department of Commerce*.

Jensen, B. W., 2015. *Numerical Analysis of Crack Propagation and Lifetime Estimation: Fracture Mechanics and Numerical Programming.* M.Sc. Master Thesis, Aalborg University Esbjerg, DK.

Lemos, R. F., 2016. *Caracterização do desvio do plano de propagação de trincas em corpos de prova CT fabricados com a liga AA 7050-T7451.* Dissertação de Mestrado em Integridade de Materiais da Engenharia, Faculdade UnB Gama/FT/Universidade de Brasília, DF.

Mandai, J. T., 2010. *Determinação dos Parâmetros Para Crescimento de Trinca em Ligas Metálicas: Modelagem e Experimentação.* Dissertação de Mestrado em Ciências Mecânicas - Universidade de Brasília, DF.

Miranda, A. C., Meggiolaro, M. A., Castro, J. T., and Martha, L. F., 2003. "Fatigue life prediction of complex 2D components under mixed-mode variable amplitude loading". *International Journal of Fatigue, 25*, 1157–1167. doi:10.1016/S0142-1123(03)00118-X

Rosa, E., 2002. *Apostila Análise da Resistência Mecânica - Mecânica da Fratura e Fadiga.* Universidade Federal de Santa Catarina, SC.

Santos, P. F., 2013. *Estudo de Técnicas de Tratamentos de Dados Experimentais para a Avaliação da curva da/dN versus ΔK: Um estudo para o aço ASTM A743 CA6NM.* Dissertação de Mestrado em Integridade de Materiais da Engenharia - Universidade de Brasília, DF.

Savioli, R. G., 2011. *Avaliação dos Parâmetros CTOD e Integral J em Juntas Soldadas Utilizando Corpos-de-prova Compactos C(T).* Dissertação de Mestrado em Engenharia - Escola Politécnica da Universidade de São Paulo, SP.

10. RESPONSIBILITY NOTICE

The authors are the only responsible for the printed material included in this paper.